UCLA
UCLA Previously Published Works

Title

An asthma-associated IL4R variant exacerbates airway inflammation by promoting conversion of regulatory T cells to TH17-like cells

Permalink

Journal

ISSN

Authors

Massoud, Amir Hossein
Charbonnier, Louis-Marie
Lopez, David
et al.

Publication Date

DOI

An asthma-associated *IL4R* variant exacerbates airway inflammation by promoting conversion of regulatory T cells to T_H17-like cells

Amir Hossein Massoud[1,2], **Louis-Marie Charbonnier**[1,2], **David Lopez**[3], **Matteo Pellegrini**[3], **Wanda Phipatanakul**[1,2], and **Talal A Chatila**[1,2]

[1]Division of Immunology, Boston Children's Hospital, Boston, MA 02115

[2]Department of Pediatrics; Harvard Medical School, Boston, MA 02115

[3]Department of Molecular, Cell and Developmental Biology, University of California, Los Angeles, CA 90095

Abstract

Mechanisms by which regulatory T (T_{reg}) cells fail to control inflammation in asthma remain poorly understood. We show that a severe asthma-associated polymorphism in the interleukin-4 receptor alpha chain (*IL4RA* R576) promotes conversion of induced T_{reg} (iT_{reg}) cells towards a T helper 17 (T_H17) cell fate. This skewing is mediated by the recruitment by IL-4Rα-R576 of the growth factor receptor-bound protein 2 (GRB2) adaptor protein, which drives IL-17 expression by activating a pathway involving extracellular signal-regulated kinase, IL-6 and STAT3. T_{reg} cell-specific deletion of *Il6ra* or *Rorc*, but not *Il4* or *Il13*, prevented exacerbated airway inflammation in *Il4ra^{R576}* mice. Furthermore, treatment of *Il4ra^{R576}* mice with a neutralizing anti-IL-6 antibody prevented iT_{reg} cell reprogramming into T_H17-like cells and protected against severe airway inflammation. These findings identify a novel mechanism for the development of mixed T_H2-T_H17 cell inflammation in genetically prone individuals, and point to interventions that stabilize iT_{reg} cells as potentially effective therapeutic strategies.

Asthma is characterized by airway hyperresponsiveness (AHR), chronic inflammation and tissue remodeling [1]. Evidence points to reduced frequency and/or suppressive activity of

Corresponding Author: Talal A. Chatila at the Division of Immunology, Boston Children's Hospital and the Department of Pediatrics, Harvard Medical School. Address: Karp Family Building, Room 10-214. 1 Blackfan Street, Boston, MA 02115, talal.chatila@childrens.harvard.edu.

FOXP3$^+$ T$_{reg}$ cells in asthma and atopic conditions [2-4]. Intense inflammation in experimental allergic asthma as well as other conditions, including rheumatoid arthritis and multiple sclerosis, may lessen T$_{reg}$ cell suppression, or redirect T$_{reg}$ cells to pro-inflammatory phenotypes [5-9]. However, the molecular basis for impaired T$_{reg}$ cell function in asthma, and the impact of T$_{reg}$ cell dysfunction on asthma severity, remain to be fully elucidated.

The cytokines IL-4 and IL-13, acting via two distinct heterodimeric IL-4 receptor complexes, play a pivotal role in asthma pathogenesis. IL-4, which binds to both the IL-4R type I (composed of the IL-4Rα and the common cytokine receptor γc chains) and II (composed of IL-4Rα and IL-13Rα1 chains) directs T$_H$2 cell differentiation. In contrast, IL-13, which exclusively binds to the IL-4R type II, promtes airway inflammation and remodeling (IL-13) [10]. Increased signaling via IL-4rα and the downstream transcription factor STAT6 exacerbates allergic airway inflammation and promotes food allergy, the latter shown to involve suppressed differentiation of allergen-specific T$_{reg}$ cells and their re-programming into T$_H$2 cell-like cells [9,11].

Polymorphisms in IL-4Rα are associated with atopy and asthma [12]. In particular, a glutamine- (Q) to arginine (R) substitution at position 576 of IL-4Rα (IL-4Rα-Q576R) has been linked to asthma exacerbation and severity [13-16]. The Q576 residue is conserved in the murine IL-4Rα chain. Its replacement by R576 in *Il4ra*^{tm2Tch} mice (also known as *Il4ra*^{R576} mice) resulted in augmented allergic airway inflammation, severe eosinophilic infiltration and increased T$_H$2 responses [17,18]. Q576 lies immediately downstream of a STAT6 binding site at Y575, one of three present in IL-4Rα [19]. Yet no discernable effect of the R576 mutation on STAT6 activation has been noted, indicating that it mobilizes alternative signaling pathways [17,20]. We here show the IL-4Rα-R576 mutation enables recruitment of the adaptor GRB2 to promote airway inflammation by a novel mechanism involving IL-4-directed iT$_{reg}$ cell differentiation towards the T$_H$17 cell lineage.

Results

Il4ra^{R576} T$_{reg}$ cell phenotype in allergic airway inflammation

Whereas allergic asthma has classically been associated with a skewed T$_H$2 cell response, a subgroup of patients with severe disease manifest a mixture of T$_H$2 and T$_H$17 cell responses in their airways [21-24]. To determine whether the IL-4Rα-R576 mutation elicits T$_H$17 airway responses *in vivo*, we employed a house dust mite (HDM)-induced model of airway inflammation [18]. *Il4ra*^{R576} mice, homozygous for the IL-4Rα-R576 mutation, exhibited severe airway inflammation as compared to control mice homozygous for the wild-type (WT) IL-4Rα-Q576 residue. The *Il4ra*^{R576} mice had increased inflammatory infiltrates and mucus production, accentuated methacholine–induced AHR and robust lung tissue eosinophilia accompanied by neutrophilia, the latter masked in earlier studies by the use of alum as an adjuvant (data not shown) (**Fig. 1a–e**) [17]. HDM treatment led to increased frequency and number of T$_{reg}$ cells in lung tissues of WT mice, but this increase was tempered in *Il4ra*^{R576} mice (**Fig. 1f**). In contrast, HDM-treated *Il4ra*^{R576} mice exhibited substantially increased frequencies and numbers of IL-17, IL-13 and IL-6 expressing CD4$^+$Foxp3$^-$ conventional T (T$_{conv}$) and CD4$^+$Foxp3$^+$ T$_{reg}$ cells as compared to WT controls (**Fig. 1g–i**). Expression of IL-17 and IL-6, but not IL-13, in *Il4ra*^{R576} T$_{conv}$ and T$_{reg}$

cells was largely overlapping (**Supplementary Fig. 1a,b**). Expression of IL-17, IL-13 and IL-5 was increased, and that of IFN-γ was decreased, in the BAL fluid of HDM-treated $Il4ra^{R576}$ mice as compared to WT controls (**Supplementary Fig. 1c**). Furthermore, HDM exposure was associated with increased expression of the T_H17 and T_H2-promoting transcription factors RORγt and GATA3, respectively, in lung T_{conv} and T_{reg} cells (**Supplementary Fig. 1d–g**). The frequencies and numbers of IL-4 producing T_{conv} and T_{reg} cells in lung tissues of HDM-treated $Il4ra^{R576}$ mice trended to increase as compared to WT controls, while those of IFN-γ cells were unchanged (**Supplementary Fig. 1h,i**).

Expression of the transcription factor Helios differentiates between natural T_{reg} (nT_{reg}) cells, which develop in the thymus and are biased towards recognition of self-antigens, from iT_{reg} cells that arise de novo in the peripheral tissues and are biased towards foreign antigens [25]. Analysis of lung tissue T_{reg} cells revealed decreased Foxp3$^+$Helios^{low} T_{reg} cells in HDM-treated $Il4ra^{R576}$ as compared to WT mice, indicative of existence of a reduced iT_{reg} cell population (**Supplementary Fig. 2a,b**). Expression of IL-17 and the T_H17 cell-associated chemokine receptor CCR6 was largely overlapping and highly enriched in T_{reg} and T_{conv} cells of HDM-treated $Il4ra^{R576}$ as compared to WT mice (**Supplementary Fig. 2c,d**). In $Il4ra^{R576}$ T_{reg} cells, IL-17 and CCR6 were almost exclusively restricted to the Foxp3$^+$Helios^{low} iT_{reg} cell population (**Supplementary Fig. 2e,f**) [26,27].

$Il4ra^{R576}$ iT_{reg} cells express IL-13, IL-17 and IL-6

TGFβ and T cell receptor (TCR) stimulation converts naïve CD4$^+$Foxp3$^-$ T cells into Foxp3$^+$ T^{reg} cells [28]. Given the increased IL-17 and IL-13 production in lung T_{reg} cells of allergen-exposed $Il4ra^{R576}$ mice, we examined in vitro-generated $Il4ra^{R576}$ iT_{reg} cells for aberrant cytokine expression and functional competency to suppress allergic airway inflammation. WT and $Il4ra^{R576}$ naïve CD4$^+$DO10.11$^+$$Rag2^{-/-}$Foxp3^{EGFP} T cells were purified by cell sorting and differentiated into T_{reg} cells in culture by stimulation with anti-CD3 and anti-CD28 mAbs and TGF β1. $Il4ra^{R576}$ CD4$^+$ T cells exhibited decreased conversion to Foxp3$^+$ T_{reg} cells as compared to WT controls, a deficit exacerbated by the addition of IL-4 to the cell cultures (**Fig. 2a,b**). Importantly, a sizeable fraction of $Il4ra^{R576}$, but not WT, CD4$^+$Foxp3$^+$ iT_{reg} cells and CD4$^+$Foxp3$^-$ T_{conv} cells expressed IL-17, which further increased by IL-4 (**Fig. 2c,d**). Anti-CD3 and anti-CD28 stimulation of $Il4ra^{R576}$ T cells induced elevated expression of IL-13 as compared to WT controls, independent of added TGF β1. IL-13 and IL-17 expression was largely non-overlapping. Addition of IL-4 induced increased IL-17 and IL-13 production in both CD4$^+$Foxp3$^+$ and CD4$^+$Foxp3$^-$ populations (**Fig. 2e,f**). In line with the above studies, expression of RORγt and GATA3 was upregulated in $Il4ra^{R576}$ iT_{reg} cells relative to WT controls (**Fig. 2e,f** and **Supplementary Fig. 3a,b**). IL-6 was co-expressed with IL-17 in $Il4ra^{R576}$ T_{reg} cells (**Fig. 2g,h**); both cytokines were IL-4-dependent, and IL-17 was also IL-6-dependent, consistent with autocrine and paracrine IL-4 production driving IL-6-dependent IL-17 expression (**Fig. 2g,h**). In contrast, IL-13 and IL-4 were increased in $Il4ra^{R576}$ T_{reg} cells in an IL-4 but not IL-6 dependent manner (**Supplementary Fig. 3c–e**). IL-4 + TGF β1 treatment induced a modest, equivalent increase in IL-9 expression in WT and $Il4ra^{R576}$ iT_{reg} cells (**Supplementary Fig. 3f–h**).

The cell surface protein neuropillin1 (Nrp1) is highly expressed on nT_{reg} cells but not iT^{reg} cells [29,30]. To determine the impact of IL-4 signaling on $Il4ra^{R576}$ nT_{reg} cells, splenic Nrp1^{high} WT and $Il4ra^{R576}$ T_{reg} cells, which are overwhelmingly nT_{reg} cells [29,30], were isolated to high purity by cell sorting (**Supplementary Fig. 4a**), and were examined for their suppressive capacity in an *in vitro* T cell proliferation assay. IL-4 treatment did not impact the suppressive function of either WT or $Il4ra^{R576}$ nT_{reg} cells (**Supplementary Fig. 4b,c**). Treatment with anti-CD3 and anti-CD28 mAbs in the presence of IL-4 induced IL-17, but not IL-13, expression in a minor population of $Il4ra^{R576}$ but not WT nT_{reg} cells that was on average 10 fold less in frequency than that noted for IL-4-treated $Il4ra^{R576}$ iT_{reg} cells (**Supplementary Fig. 4d,e**). Also, treatment of naïve $Il4ra^{R576}$ T_{conv} cells with IL-4 failed to induce IL-17 expression in the absence of TGF β1 (**Supplementary Fig. 4f,g**). These results indicated that the capacity of $Il4ra^{R576}$ T_{reg} cells to express IL-17 in response to IL-4 treatment is largely restricted to the iT_{reg} cell population.

Impaired function of $Il4ra^{R576}$ T_{reg} cells

To assess suppressive capacities of $Il4ra^{R576}$ vs. WT iT_{reg} cells, we employed an adoptive transfer model. iT_{reg} cells were derived from naïve splenic CD4$^+$ T cells of WT and $Il4ra^{R576}Thy1.1^+DO10.11^+Rag2^{-/-}Foxp3^{EGFP}$ mice and adoptively transferred to OVA-sensitized $Il4ra^{R576}Thy1.2^+$ mice, which were then challenged with aerosolized OVA and analyzed (**Supplementary Fig. 5a**). WT iT_{reg} cells almost completely abrogated OVA–induced tissue inflammation, goblet cell hyperplasia, AHR, eosinophilia neutrophilia and lymphocytosis in lungs of recipient $Il4ra^{R576}$ mice. They also suppressed IL-17 and IL-13 expression in the recipient lung T_{conv} and T_{reg} cells. In contrast, $Il4ra^{R576}$ iT_{reg} cells failed to do so (**Supplementary Fig. 5b–f**). Unlike the transferred WT iT_{reg} cells, up to a third of donor $Il4ra^{R576}$ iT_{reg} cells lost their EGFP expression to become $exiT_{reg}$ cells that expressed either IL-17 or, less frequently, IL-13, consistent with heightened instability (**Supplementary Fig. 5g–j**).

We utilized CCR6 as a marker of T_{reg} cells committed towards the T_H17 cell lineage to examine their functional, epigenetic and transcriptional profiles. CCR6$^+$ $Il4ra^{R576}$ T_{reg} cells isolated from OVA-sensitized and challenged mice exhibited decreased methylation of the *Foxp3 CNS2* locus, indicative of decreased T_{reg} cell phenotypic stability (**Fig. 3a,b**). They also exhibited profoundly decreased suppressive function in an *in vitro* T cell proliferation assay as compared to CCR6$^-$ WT and CCR6$^-$ $Il4ra^{R576}$ counterparts (**Fig. 3c**). Transcriptional profiling revealed increased expression in CCR6$^+$ $Il4ra^{R576}$ T_{reg} cells of genes associated with a T_H17 cell signature, including Rorc, Ccr6, Il23r, Il17a, Il17f, Il1r1, Nr1d1, Cstl, and *Ahr* (**Fig. 3d** and **Supplementary Data Set 1**) [26,31-33]. To determine whether the T_H17 cell-like T_{reg} cells in the lungs of allergen treated $Il4ra^{R576}$ mice gave rise to Foxp3$^-$ T_H17 cells, we employed a lineage tracing approach using a *Rosa26* Stop-flox YFP reporter ($R26^{YFP}$) crossed with a *Foxp3*-directed Cre recombinase ($Foxp3^{EGFPCre}$) on WT and $Il4ra^{R576}$ background. $Il4ra^{R576}Foxp3^{EGFPCre}R26^{YFP}$ and control $Foxp3^{EGFPCre}R26^{YFP}$ mice were either sham or OVA sensitized than challenged with aerosolized OVA. CCR6 and cytokine expression was examined in T_{reg} (EGFP$^+$YFP$^+$), exT_{reg} (EGFP$^-$YFP$^+$) and CD4$^+$ T^{conv} cells (EGFP$^-$ YFP$^-$). We found markedly increased frequencies of EGFP$^-$YFP$^+$ exT_{reg} cells in the lungs of OVA-sensitized and challenged

Il4ra^{R576}*Foxp3*^{EGFPCre}*R26*^{YFP} relative to controls, indicative of heightened T$_{reg}$ cell instability (**Fig. 3e**). Furthermore, about half of those exT$_{reg}$ cells expressed IL-17 and CCR6, consistent of their differentiation into T$_H$17 cells. In contrast, expression of IL-13 by exT$_{reg}$ cells was modest (**Fig. 3f,g**). Together, IL-17 producing T$_{reg}$ and exT$_{reg}$ cells accounted for 35–40% of the total CD4$^+$IL-17$^+$ and CD4$^+$CCR6$^+$ T cells in the lungs of OVA-treated *Il4ra*^{R576}*Foxp3*^{EGFPCre}*R26*^{YFP} mice but less than 3% in similarly treated WT controls (**Fig. 3h**). These results indicated that *Il4ra*^{R576}–driven T$_{reg}$ cell instability and T$_H$17-cell-like programming in the context of allergic airway inflammation ultimately leads to T$_{reg}$ cell transformation into T$_H$17 cells.

Recruitment of GRB2 to IL-4Rα-pY575 activates MAPK

We noted that the R576 substitution rendered the sequence at Y575 (574-GpYREF-578) homologous to a previously reported consensus sequence for high specificity binding of the src homology 2 (SH2) domain of the adaptor protein GRB2 (pY-K/R-N-I/L) [34]. Consistent with this prediction, GRB2 and the GRB2-associated binding protein 2 (GAB2) were detected by immunoblotting in IL-4Rα immunoprecipitates derived from IL-4–treated *Il4ra*^{R576} but not WT T cells (**Fig. 4a**). Furthermore, GRB2 was recovered from mouse splenocyte and human PBMC lysates using biotinylated 15 amino acid murine and human IL-4Ra peptides containing phosphorylated Y575 residue and R576 (pY575R576) but not the Q576 residue (pY575Q576) (**Fig. 4b** and **Supplementary Fig. 6a**). Both murine and human pY575R576 peptides demonstrated a modest decrease in STAT6 binding compared to pY575Q576. Together, these data indicated that the R576 substitution altered the specificity of pY575 towards binding GRB2 versus STAT6.

Receptor-bound GRB2 activates the guanine nucleotide exchange factor Son of Sevenless (SOS), which in turn activates the mitogen-activated protein kinase (MAPK) kinase cascade [35]. Consistent with GRB2 recruitment and activation, IL-4 stimulation of *Il4ra*^{R576} but not WT splenocytes increased the phosphorylation of MAPKs, including the c-Raf, MKK3/6, ERK1/2 and p38 MAPK (**Fig. 4c** and **Supplementary Fig. 6b,c**). Activation of these kinases was inhibited by GRB2-specific but not scrambled small interfering RNA (siRNA) (**Fig. 4c**). ERK1/2 but not p38 MAPK activation was suppressed by treatment with a c-Raf inhibitor, pointing to two downstream cascades branching out from GRB2, one involving c-Raf–ERK1/2 and the other P38 MAPK and its activator MKK3/6 (**Supplementary Fig. 6d**). IL-4 activated *Il6* transcription in several cell types, including bone marrow derived macrophages (BMDM), splenocytes and purified T cells in a GRB2-ERK1/2 cascade-dependent manner, evidenced by inhibition of *Il6* transcripts by *Grb2* siRNA and a MAPK kinase (MEK) inhibitor, which inhibits ERK1/2 activation, but not by a P38 MAPK inhibitor (**Fig. 4d,e** and **Supplementary Fig. 6e**). IL-4 induced ERK1/2-dependent phosphorylation of NF-κB p65, known transcriptional activators of *Il6*, and mobilized p65 and C/EBPβ to the *Il6* promoter [36,37] (**Fig. 4f** and **Supplementary Fig. 6f**). The activation of NF-κB was inhibited by MEK inhibitor treatment (**Supplementary Fig. 6g**).

IL-6-dependent STAT3 activation in *Il4ra*[R576] cells

IL-6 skews iT$_{reg}$ cell differentiation towards the T$_H$17 cell lineage in a STAT3-dependent manner [38,39]. Consequent to IL-4Rα-R576-mediated IL-6 production, differentiating *Il4ra*[R576] iT$_{reg}$ cells exhibited increased STAT3 activation as compared to WT controls, and this STAT3 activation that was IL-4 and IL-6 dependent (**Fig. 4g**). Analysis of IL-4 induced STAT3 activation in *Il4ra*[R576] naïve CD4$^+$ T cells revealed delayed phosphorylation of STAT3 that started at 30 min post stimulation and progressively increased over time. It was completely abrogated by treatment with an anti–IL-6 mAb, indicating that IL-4–induced STAT3 phosphorylation proceeded by IL-4-mediated IL-6 production. In contrast, activation by IL-4 of STAT6, and by IL-6 of STAT3, was indistinguishable between WT and *Il4ra*[R576] T cells (**Supplementary Fig. 7a–c**).

We next analyzed the role of GRB2-activated MAPK cascades in iT$_{reg}$ cell skewing towards a T$_H$17 versus T$_H$2 cell phenotype. Treatment of differentiating *Il4ra*[R576] iT$_{reg}$ cells with MEK inhibitor or anti–IL-6 mAb, but not p38 MAPK inhibitor, rescued the decreased iT$_{reg}$ cell differentiation, decreased IL-6 levels in culture, and blocked IL-17 expression in differentiating iT$_{reg}$ cells and in CD4$^+$ T$_{conv}$ cells present in the same co-cultures while sparing IL-13 (**Fig. 4h–j and Supplementary Fig. 6h–j**). Treatment with p38 MAPK inhibitor blocked IL-13 but not IL-17 expression, consistent with the role of p38 in the upregulation of *Il13* gene transcription by a GATA3-dependent mechanism [40], while treatment with anti–IL-4 mAb blocked both (**Fig. 4i,j** and **Supplementary Fig. 6i,j**). Thus the two branches of MAPK signaling downstream of IL-4Rα–R576 mediate activation of distinct T$_H$ cell cytokine programs.

Whereas T cells express only the type I IL-4R, which responds to IL-4, bone marrow derived macrophages (BMDM) also express the type II receptor, which responds to IL-4 and IL-13. Stimulation of *Il4ra*[R576] but not WT BMDM with IL-4 or IL-13 induced a similar profile of delayed, sustained STAT3 activation. In contrast, STAT3 was similarly activated in IL-6–treated WT and *Il4ra*[R576] BMDM (**Supplementary Fig. 7d,e**).

Expression of transcripts encoding CCL11, which mediates tissue eosinophil recruitment, is markedly upregulated in the airways of allergen-challenged *Il4ra*[R576] mice [17]. *Ccl11* transcripts were greatly increased in IL-4-treated *Il4ra*[R576] BMDM as compared to WT controls (**Supplementary Fig. 7f**). *Ccl11* transcriptional activation by IL-4/IL-13 is normally mediated by STAT6, while that by IL-17 and IL-9 is mediated by STAT3 [41-43]. Chromatin immunoprecipitation (ChIP) assays revealed that whereas STAT6 bound equally well to the *Ccl11* promoter in IL-4-treated WT and *Il4ra*[R576] BMDM, STAT-3 was selectively recruited to the *Ccl11* promoter in *Il4ra*[R576] BMDM in an IL-6-dependent manner (**Supplementary Fig. 7g**). Knockdown of STAT3 by siRNA treatment abrogated the increase in *Ccl11* transcription in IL-4-treated *Il4ra*[R576] BMDM, reducing it to levels similar to those of WT controls (**Supplementary Fig. 7h,i**). Thus dual STAT6-STAT3 activation by IL-4Rα-R576 may promote tissue eosinophilia by super-inducing *Ccl11* transcription.

iT$_{reg}$ cells of humans expressing *IL4R*^{R576} produce IL-17

We examined *in vitro* iT$_{reg}$ cell differentiation in prospectively recruited healthy and asthmatic subjects who were either WT (*IL4R*$^{Q576/Q576}$), heterozygous (*IL4R*$^{Q576/R576}$) or homozygous for the mutant allele (*IL4R*$^{R576/R576}$). The gating strategy in these studies is outlined in **Figure 5a**. In healthy subjects, whose demographics are detailed in **Supplementary Table 1**, naïve heterozygous and homozygous mutant T$_{conv}$ cells differentiated to iT$_{reg}$ cells at lower frequencies as compared to WT T cells, especially in the presence of IL-4 (**Fig. 5b**). The deficit in iT$_{reg}$ conversion was rescued by treatment with an anti–IL-6 mAb. The differentiated iT$_{reg}$ cells and CD4$^+$ T$_{conv}$ cells present in the same co-cultures produced increased amounts of IL-17 as assessed by flow cytometric analysis and by ELISA, which was further upregulated by IL-4 treatment but abrogated by anti–IL-6 mAb (**Fig. 5b,d**). IL-13 expression was significantly increased in activated T cells of subjects carrying the mutant allele independent of their differentiation into iT$_{reg}$ cells, mirroring the findings in murine *Il4ra*^{R576} T cells (**Fig. 5b,d**).

We also examined the differentiation and cytokine expression of iT$_{reg}$ cells in prospectively recruited asthmatics as a function of *IL4R* genotype. The demographics, *IL4R* genotype and disease severity classification of asthmatic subjects are described in **Supplementary Table 2**. Whereas there were no differences in age and sex distribution between asthmatics bearing the WT allele versus those heterozygous and homozygous for the mutant allele, the latter subjects exhibited increased asthma severity, in agreement with previously published reports (**Supplementary Table 2**) [13-16]. Heterozygous and homozygous mutant, but not WT, iT$_{reg}$ cells of asthmatics also exhibited IL-6–dependent decreased differentiation and increased IL-17 production (**Fig. 5c,d**). IL-13 expression was upregulated in activated T$_{conv}$ and in iT$_{reg}$ cells of asthmatics regardless of their genotype, although ELISA assays revealed its increased production by cells carrying the mutant allele (**Fig. 5c,d**). Analysis of peripheral blood mononuclear cells (PBMC) revealed a modest but significant decrease in circulating total T$_{reg}$ cells in asthmatics homozygous for the *IL4R*^{R576} allele. This decrease was restricted to the Foxp3$^+$Helios^{low} (iT$_{reg}$) cell population, which also manifested a selective increase in CCR6 expression, echoing the results found in *Il4r*^{R576} mice (**Fig.5 e,f; Supplementary Fig. 8**). Importantly, the frequency of IL-17–expressing CD4$^+$ T$_{conv}$ and T$_{reg}$ cells was selectively increased in subjects either heterozygous or homozygous for *IL4R*^{R576}. IL-13 expression was modestly increased in CD4$^+$ T$_{conv}$ and T$_{reg}$ cells of PBMC of subjects homozygous for *IL4R*^{R576} consistent with heightened T$_H$17 and T$_H$2 responses (**Fig. 5g**). These results established that IL-4–driven acquisition by iT$_{reg}$ cells of a T$_H$17 cell-like phenotype is an attribute that segregates with the IL4-Rα-R576 mutation.

Il4ra^{R576} T$_{reg}$ cell phenotype change impacts airway inflammation

To determine whether the acquisition by lung *Il4ra*^{R576} T$_{reg}$ cells of a T$_H$17 cell-like phenotype contributed to exaggerated airway inflammation, we examined the consequences of T$_{reg}$ cell-specific deletion of *Rorc*, which encodes the T$_H$17-promoting transcription factor RORγt, on airway inflammation [44]. T$_{reg}$ cell specific deletion was effected by crossing mice expressing a floxed *Rorc* allele with mice expressing *Foxp3*^{YFPCre}, a Cre recombinase under control of the *Foxp3* locus (**Supplementary Fig. 9a,b**). T$_{reg}$ cell-specific deletion of *Rorc* in *Il4ra*^{R576} mice (*Il4ra*^{R576}*Foxp3*^{YFPCre}*Rorc*$^{/}$) decreased airway

inflammation, mucus production and AHR upon OVA sensitization and challenge to an extent sufficient to resemble WT controls that were either sufficient or deficient in *Rorc* (*Foxp3*[YFPCre] and *Foxp3*[YFPCre]*Rorc* [/] , respectively), whose aforementioned responses were not significantly different (**Fig. 6a–c**). It also led to a sharp decrease in lung tissue neutrophilia, lymphocytosis and to a lesser extent eosinophilia. In contrast, total and OVA-specific serum IgE concentrations were marginally decreased (**Fig. 6d,e**). *Rorc* deletion rescued the decrease in lung tissue T_{reg} cells in OVA-sensitized and challenged *Il4ra*[R576] mice (**Supplementary Fig. 9c**). It abolished IL-17 expression and normalized CCR6 expression in *Il4ra*[R576] T_{reg} cells, and normalized IL-17 and CCR6 expression in $CD4^+$ T_{conv} cells. In contrast, IL-13 expression was unaffected in *Il4ra*[R576]*Foxp3*[YFPCre]*Rorc* [/] T_{reg} cells and marginally so in $CD4^+$ T_{conv} cells (**Fig. 6f–i** and **Supplementary Fig. 9d–h**). Virtually identical results were obtained upon *Il4ra*[R576] T_{reg} cell-specific deletion of *Il6ra*, encoding IL-6Rα chain, consistent with the requirement for IL-4-induced IL-6 production in programming T_H17 cell-like T_{reg} cells **(Supplementary Fig. 10)**. Similarly, treatment with anti–IL-6 mAb suppressed airway inflammation and AHR in HDM-treated *Il4ra*[R576] mice, abrogated airway neutrophilia and profoundly inhibited the airway eosinophilia. It normalized lung tissue T_{reg} cell numbers and prevented iT_{reg} cell reprograming into T_H17-like cells, and it inhibited T_H2 and T_H17 cytokine production and the increased IgE response (**Supplementary Fig. 11**). In contrast, treatment with an anti–IL-17 mAb was less effective in suppressing HDM-induced airway inflammation in *Il4ra*[R576] mice. It partially decreased tissue inflammation and AHR, normalized airway neutrophilia and inhibited IL-17 production. However, it only marginally decreased airway eosinophilia. It failed to suppress IgE or T_H2 cytokine production or to rescue reduced T_{reg} cell numbers in lung tissues (**Supplementary Fig. 12**). Treatment with an anti-CCL11 mAb, while inhibiting dysregulated airway eosinophilia and CCL11 production in HDM-treated *Il4ra*[R576] mice, did not suppress tissue inflammation, airway neutrophilia, T_H2 and T_H17 cytokine or IgE production, nor did it rescue ineffective T_{reg} cell generation in lung tissues (**Supplementary Fig. 13**). Unlike the case of *Rorc* and *Il6ra*, combined T_{reg} cell-specific deletion of *Il4 and Il13* had no significant effect on airway inflammation, AHR, or lung tissue neutrophilia in OVA-sensitized and challenged *Il4ra*[R576] mice despite decreased total eosinophilia and total and OVA-specific IgE responses. It failed to rescue the decrease in lung tissue T_{reg} cells in inflamed *Il4ra*[R576] mice. While it completely suppressed IL-13 expression in T_{reg} cells, and decreased it in $CD4^+$ T_{conv} cells, it left unaltered IL-17 expression in either cell population (**Supplementary Fig. 14**).

For comparison, we employed *Il4ra*[F709] mice, homozygous for a Y709F substitution that inactivates the immunotyrosine inhibitory motif of the IL-4Rα chain and consequently augments STAT6 activation [11]. This mutation, which models human IL-4Rα polymorphisms that promote STAT6 activation, results in exaggerated allergic airway inflammation due to dysregulated T_H2 immunity [11,45,46]. *Il4ra*[F709] T_{reg} cells undergo T_H2 cell-like reprogramming that plays a fundamental role in mediating the exaggerated allergic phenotype [9]. Unlike *Il4ra*[R576] mice, T_{reg} cell-specific deletion of *Il4/Il13* in *Il4ra*[F709] mice normalized their airway inflammation, AHR, and tissue eosinophilia and decreased their total and OVA-specific IgE responses. It reversed T_{reg} cell T_H2 cell-like reprogramming, evidenced by abolishment of their heightened IL-13 expression, and reduced IL-13

production by CD4$^+$ T$_{conv}$ cells, without affecting the low IL-17 expression in CD4$^+$ T$_{conv}$ and T$_{reg}$ cells (**Supplementary Fig. 15**). Thus, the *Il4ra*^{R576} and *Il4ra*^{F709} augment airway inflammation by two distinct mechanisms: one eliciting a T$_H$17 and the other a T$_H$2 cell-like reprograming of T$_{reg}$ cells.

Discussion

Our studies elucidate a novel mechanism for the development of mixed T$_H$2 and T$_H$17 cell responses relevant to asthma and other allergic inflammatory diseases. By activating an additional branch of IL-4R signaling initiated by the adaptor protein GRB2, an IL-4Rα polymorphism associated with asthma exacerbations and severity potentiates T$_H$17 and to a lesser extent T$_H$2 responses. Importantly, IL-4-induced GRB2 recruitment mediates MAPK-dependent autocrine IL-6 signaling in T cells, which redirects TGF β-dependent iT$_{reg}$ cell differentiation towards the T$_H$17 cell lineage. Deletion of *Il6ra* or *Rorc* in T$_{reg}$ cells or treatment with an anti–IL-6 mAb protected against the deleterious effects of IL-4Rα-R576 on airway inflammation, prevented iT$_{reg}$ cell reprogramming towards the T$_H$17 lineage and normalized the T$_H$17 cell response, confirming the centrality of iT$_{reg}$ cell acquisition of a T$_H$17 cell-like phenotype in mediating disease exacerbation by this polymorphism.

In mouse models, IL-17 induces steroid-resistant airway inflammation and neutrophilic infiltration [27,47,48]. However, while anti–IL-17 mAb treatment suppressed lung tissue neutrophilia and neutralized IL-17 in the airways of *Il4ra*^{R576} mice, it only partially ameliorated the augmented AHR and tissue inflammation and failed to normalize the T$_{reg}$ cell response or suppress T$_H$17/T$_H$2 polarization. Thus, the efficacy of interventions such as T$_{reg}$ cell-specific deletion of *Rorc or Il6ra* or treatment with anti–IL-6 mAb relates not simply to their suppression of IL-17 production but more fundamentally to their stabilization of the iT$_{reg}$ cell response, resulting in better control of airway inflammation. Studies on *Il4ra*^{R576} and *Il4ra*^{F709} mice revealed two distinct modes of pathogenic iT$_{reg}$ cell programming relevant to airway inflammation. The former involved GRB2-dependent iT$_{reg}$ cell programming towards a T$_H$17-cell like phenotype, while the latter involved STAT6-dependent programming towards a T$_H$2 cell-like phenotype [9]. T$_{reg}$ cell-specific deletion of *Il6ra* or *Rorc* in *Il4ra*^{R576} mice and *Il4-Il13* in *Il4ra*^{F709} mice reduced airway inflammation in the respective strain back to levels associated with the WT *Il4ra* allele. *Il4ra*^{R576} and *Il4ra*^{F709} mice model mixed T$_H$2-T$_H$17 and T$_H$2 cell-high asthma inflammatory mechanisms, or endotypes, respectively [49-51]. Both models would indicate that acquisition of iT$_{reg}$ cells of a T$_H$17 or a T$_H$2 cell-like program plays a fundamental role in the pathogenicity of the respective allele in airway inflammation. Accordingly, pro-asthmatic IL-4R polymorphisms may promote distinct asthma endotypes (T$_H$2 cell-high versus mixed T$_H$2-T$_H$17 cell inflammation) by directing iT$_{reg}$ cells differentiation towards the respective T$_H$ cell program.

Our results indicate that IL-4-directed and IL-6-dependent subversion of *IL4R*^{R576} iT$_{reg}$ cells into a T$_H$17 like cells may play a critical role in asthma severity associated with this allele. Blocking the IL-4R or IL-6R pathways may prevent the subversion of allergen-specific iT$_{reg}$ cells into T$_H$2 and/or T$_H$17 like cells, respectively, and provide personalized therapeutic approaches to tolerance re-establishment in asthma [52,53].

Online Methods

Animals

BALB/cByJ (WT) and all the following strains, except where indicated, were obtained from or rederived at the JAX lab. *C.129X1-Il4ra*[tm2.1Tch] (*Il4ra*[R576]), *C.129X1-Il4ra*[tm3.1Tch] (*Il4ra*[F709]), and C.Cg-*Foxp3*[tm2Tch]/J (*Foxp3*[EGFP]) have been previously described [11,17,54]. NOD/ShiLt-Tg(*Foxp3*[EGFP-cre])1cJbs/J (*Foxp3*[EGFPCre]) were backcrossed 12 generations on BALB/cBYJ [55]. *C.129P2(Cg)-Il4-Il13*[tm1.1Lky] (*Il4-Il13*^{fl/fl}) mice were crossed with *Il4ra*[R576] and *Il4ra*[R576]*Foxp3*[EGFPCre] mice [56]. *DO11.10*[+]*Rag2*^{−/−} mice were obtained from Taconic Farms (Hudson, NY) and were crossed with *Thy1.1*[+]*Foxp3*[EGFP] and *Thy1.1*[+]*Il4ra*[R576] mice to generate *Thy1.1*[+]*DO11.10*[+]*Rag2*^{−/−}*Foxp3*[EGFP] and *Thy1.1*[+]*Il4ra*[R576]*DO11.10*[+]*Rag2*^{−/−}*Foxp3*[EGFP] mice. ROR-gtf/fB6(Cg)-*Rorc*[tm3Litt]/J (*Rorc*^{fl/fl}), B6;SJL-*Il6ra*[tm1.1Drew]/J (*Il6ra*^{fl/fl}), B6.129(Cg) *Foxp3tm4(YFP/cre)Ayr*/J) (*Foxp3*[YFPCre]) and *Il4ra*[R576] C57BL/6 congenic were crossed to generate *Il4ra*[Q576]*Foxp3*[YFPCre], *Foxp3*[YFPCre]*Rorc*[/] and *Il4ra*[R576]*Foxp3*[YFPCre]*Rorc*[/]. BALB/c *Il4ra*[R576] mice were crossed to congenic *Foxp3*[EGFPCre]*Rosa26*[YFPCre] mice to generate *Il4ra*[R576] *Foxp3*[EGFPCre]*Rosa26*[YFPCre] [57,58]. Male and female mice, age 5-7 weeks, were employed in experiments in equal proportions. Mice were bred and maintained under specific pathogen-free conditions and used under protocols approved by the Institutional Animal Care and Use Committee at Boston Children's Hospital.

Flow cytometry

Antibodies against the following murine antigens were used for flow cytometric analyses: IL-4 (clone 11B11, 1:300 dilution), Siglec-F (E50-2440, 1:300), Phospho-Stat3 (pY705, 1:50), Phospho-Stat6 (pY641, 1:50) (BD Biosciences), Thy1.2 (30-H12, 1:500), Foxp3 (FJK-16S, 1:300), DO11.10 (KJ1-26, 1:500), IFN-γ (XMG1.2, 1:300), IL-13 (eBio13a, 1:300), GATA3 (TWAJ, 1:200), RORγt (AFKJS-9, 1:200), Helios (22F6, 1:200), CD25 (PC61.5, 1:500), CTLA4 (UC10-4B9, 1:200), CD11c (30-f11, 1:500), CD11b (M1/70, 1:500) (eBioscience), CD4 (RM4-5, 1:500), CD3 (145-2C11, 1:500), IL-17 (TC11-18H10.1, 1:200), IL-6 (MP5-20F3, 1:200), GR-1 (RB6-8C5, 1:500), CCR6 (29-2L17, 1:300) and CD45 (30-F11, 1:300) and CD304 (Neuropilin-1; 3E12, 1:200) (Biolegend). Antibodies against the following human antigens were used: CD4 (RPA-T4, 1:300), Foxp3 (236A/E7, 1:200), IL-13 (JES10-5A2, 1:200), IL4 (MP4-25D2, 1:400) (eBioscience), IL-17A (BL168, 1:200), Helios (22F6, 1:200), CCR6 (G034E3, 1:200) (Biolegend). The specificity and optimal dilution of each antibody was validated by testing on appropriate negative and positive controls or otherwise provided on the manufacturer's website. Intracellular cytokine staining was performed as previously described [9]. Cells were routinely excluded from the analysis based on the staining of eFluor 780 Fixable Viability Dye (eBioscience). Stained cells were analyzed on a BD LSRFortessa cell analyzer (BD Biosciences) and data were processed using Flowjo (Tree Star Inc.).

Cell purification

Cell suspensions were enriched in CD4^{+} T cells by Magnetic-activated cell sorting (MACS) negative selection (Miltenyi Biotec) and further sorted by a fluorescence-activated cell

sorting (FACS) on a FACSAria II (BD Biosciences) based on CD4 and EGFP (Foxp3) expression.

Mouse allergic sensitization and antibody treatment

Mice were sensitized to ovalbumin (OVA) (Grade V; Sigma Aldrich) by intraperitoneal injection of 100 µg of OVA in 100 µL of PBS and then boosted 2 weeks later with a second intraperitoneal injection of OVA in PBS. Control mice were sham sensitized and boosted with PBS alone. Starting on day 29, both OVA- and sham-sensitized mice were challenged with aerosolized OVA at 1% delivered through a Schuco 2000 nebulizer (Allied Health Care Products) for 30 minutes daily for 3 days. Mice were euthanized on day 32 post sensitization and analyzed [18]. For House Dust mite (HDM)– induced allergic airway inflammation, mice received 20 µg of lyophilized *Dermatophagoides pteronyssinus* (DP) extract in 100 µl of PBS intranasally for 3 days at the start of the protocol and then challenged with the same dose of DP extract on days 15 to 17. Mice were euthanized on day 18 and analyzed for measures of airway inflammation [18]. In some experiments at day 15 to 17 monoclonal anti-IL-6 (MP5-20F3, BioXCell) or anti-IL-17 (17F3, BioXCell) antibodies or the isotype-matched control antibodies (BioXCell) were administered intra-tracheally (100 µg/day), 30 min prior to allergen challenge.

Preparation of cell suspensions from lung tissues

Lungs were removed, minced, and incubated for 45 minutes at 37'C in collagenase (Sigma-Aldrich) (0.5 mM in PBS) and passed through a 40-mm strainer. Single-cell suspensions were resuspended in RPMI medium (Invitrogen)

Measurement of airway tissue and functional responses

Paraffin-embedded lungs sections were stained with periodic acid–Schiff (PAS) as previously described [59]. Lung inflammation was scored for cellular infiltration around the airways: 0, no infiltrates; 1, few inflammatory cells; 2, a ring of inflammatory cells 1 cell layer deep; 3, a ring of inflammatory cells 2 to 4 cells deep; and 4, a ring of inflammatory cells greater than 4 cells deep [11]. The number and distribution of goblet cells was assessed by using PAS staining of mucin granules. Individual airways (bronchi/bronchioles) were scored for goblet cell hyperplasia according to the following scale: 0, no PAS-positive cells; 1, less than 5% PAS-positive cells; 2, 5% to 10% PAS-positive cells; 3, 10% to 25% PAS-positive cells; and 4, greater than 25% PAS-positive cells [11]. Allergen-induced airway hyperreactivity (AHR) was measured, as previously described [18]. Anesthetized mice were exposed to doubling concentrations of aerosolized acetyl-β-methacholine (Sigma-Aldrich) by using a Buxco small-animal ventilator (Data Sciences International). The relative peak airway resistance for each methacholine dose, normalized to the saline baseline, was calculated.

In Vitro iT$_{reg}$ cell differentiation

Sorted naive CD4$^+$CD62L$^+$Foxp3^{EGFP-} T cells (1 × 10^6/ml) were cultured with plate-bound anti-CD28 (5 µg/ml, Biolegend), anti-CD3 (5 µg/ml, Biolegend), recombinant TGF β1 (5 ng/ml, R&D Systems), with or without murine recombinant IL-4 (10 ng/ml) (Perpotech),

anti-IL-4 (11B11, 10 μg/ml) (Biolegend) or anti-IL-6 mAb (MP5-20F3, 10 μg/ml) (Biolegend), mitogen activated protein kinase kinase (MEK) inhibitor PD98059 (50 μM, Sigma-Aldrich) or P38 inhibitor IV (10 μM, Sigma-Aldrich). After 4 days, the induced iT$_{reg}$ cells were analyzed by flow cytometry for Foxp3 expression and intracellular cytokines production and/or re-sorted on the basis of EGFP fluorescence.

Differentiation of Bone marrow derived macrophages (BMDM)

BMDM were generated from bone marrow cells collected from femurs were cultured in complete medium supplemented with 10 ng/mL recombinant murine M-CSF (PeproTech) for 10 days. The medium was changed every other day. Adherent BMDM were harvested at day 10. Purity of BMDM was verified by using flow cytometry and was greater than 90%, as determined by using CD11c and F/480 staining.

Quantitative real-time PCR

RNA was extracted from treated cells, as mentioned in the figure legends, using Quick-RNA MiniPrep kit (Zymo Research) according to the manufacturer protocol. Reverse transcription was performed with the SuperScript III RTPCR system (Invitrogen) and quantitative real-time reverse transcription (RT)-PCR with Taqman® Fast Universal PCR master mix, internal house keeping gene mouse (GAPDH VIC-MGB dye) and specific target gene primers for murine *Il6, Ccl11*, *Rorc* or *Il4* genes, as indicated (FAM Dye) (Applied Biosystems) on Step-One-Plus machine. Relative expression was normalized to GAPDH and calculated as fold change compared to un-stimulated WT cells.

Immunoblotting and immunoprecipitation

Cells were treated with medium alone or medium with IL-4 (10 ng/ml) for the indicated times, lysed with the lysis buffer (25 mM Tris-HCl (pH 7.5), 150 mM NaCl, 5 mM EDTA (pH 8), 1 mM Na$_3$VO$_4$, 0.5% NP-40, 1 × diluted protease inhibitor cocktail (Sigma-Aldrich). Whole cell lysates were resolved by SDS/PAGE and transferred to PVDF membrane (Thermo Scientific) for immunoblotting analysis [59]. Immunoprecipitates were derived from cell lysates using the indicated antibodies and Protein G superparamagnetic beads (Life Technologies). Following overnight incubation, the immunoprecipitates were eluted from the beads by boiling in gel loading buffer and subjected to immunoblotting as previously described [59]. The following antibodies were used: GRB2 (clone 4C6-H6, 1:1000 dilution), p-GAB2 (Ser159, EP369Y, 1:1000) p-ERK1/2 (Thr202/Tyr204, D13.14.4E, 1:1000), ERK1/2 (p44/42 MAP Kinase, 137F5, 1:1000), STAT6 (D3H4, 1:1000), STAT3 (D3Z2G, 1:1000) p-c-Raf (Ser338, 56A6, 1:1000), c-Raf (D5X6R, 1:1000), p-P38 (Thr180/Tyr182, D3F9, 1:1000), P38 (D13E1, 1:1000), p-MKK3/6 (Ser189/Ser207, 22A8, 1:1000), MKK3 (D4C3, 1:1000), NF-κB p-p65 (Ser536, 93H1, 1:1000), NF-κB p65 (D14E12, 1:1000) (all obtained from Cell Signaling Technology), C/EBPβ (C-190, 1:1000) (Santa Cruz Biotechnology) and anti-IL-4Rα (CD124) mAb (mIL-4R-M1, 1:1000) (BD Pharmingen). The specificity and optimal dilution of each antibody was validated by testing on appropriate negative and positive controls or otherwise provided on the manufacturer's website.

Chromatin immunoprecipitation (ChIP)

ChIP was performed with Agarose ChIP Kit (Pierce) and antibodies toward STAT3 (D3Z2G, 1:100), STAT6 (D3H4, 1:100), c-Jun (AP-1, 1:100) and NF-κB p65 (D14E12, 1:100) (all obtained from Cell Signaling Technology), C/EBPβ (C-190, 1:100) (Santa Cruz Biotechnology) and the respective isotype control antibodies on 2×10^6 cells starved for 3 hr and treated with medium alone or with IL-4 (10 ng/ml, 2 hrs). The DNA from sample and input was amplified by RT-PCR (40 cycles), using the following primers specific for the *Il6* promoter; 5'-AGTGGTGAAGAGACTCAGTG-3' (forward) and 5'-GGCAGAATGAGCCTCAGA-3' (reverse) and specific primers for the *Ccl11* promoter; 5'-CTTCATGTTGGAGGCTGAAG-3' (forward) and 5'-GGATCTGGAATCTGGTCAGC-3' (reverse). Results presented as the ratio of the cycling threshold value of immunoprecipitated DNA to that of input DNA.

siRNA–mediated knockdown of GRB-2

Cells were transfected for 72 hr with scrambled small interfering RNA (siRNA) or *Grb2* siRNA I (Cell Signaling Technology) for inhibition of GRB2 expression (50 nM /10^6 cells). *Stat3* siRNA I (Cell Signaling Technology) was used for STAT3 inhibition. Lipofectamine 3000 reagent (Life Technologies) was used to increase the efficiency of transfection (0.5 nmol/L).

IgE and cytokine ELISA assays

Total mouse serum IgE was measured by ELISA using Mouse IgE ELISA Ready-SET-Go kit (eBioscience). OVA-specific IgE was measured by a modified assay such that the plates were coated overnight with 200 μg/ml OVA rather than anti-IgE capture antibody and the rest of the test was similar to the total serum IgE ELISA assay. Mouse IL-4, IL-5, IL-13, IL-17 IFN-γ and Eotaxin cytokines were analyzed in BAL fluids collected from mice using eBioscience ELISA kits, according to the manufacturer's protocol. Human IL-13 and IL-17 were analyzed in culture supernatants of human peripheral blood cells activated with anti-CD3 + anti-CD28 mAbs in the absence or added presence of TGF β or TGF β + IL-4 using eBioscience ELISA kits.

Peptide affinity pull-down experiment

The following biotinylated peptides, corresponding to amino acids 569-583 and 569-584 of the human and mouse IL-4Ra, respectively, and encompassing either WT (Q) or mutant (R) at position 576 were used: Y575Q576: Biotin-SAPTSGYQEFVHAVE (human), Biotin-PAPAGGYQEFVQAVKQ; pY575Q576 (mouse); pY575R576: Biotin-SAPTSGpYQEFVHAVE (human), PAPAGGpYQEFVQAVKQ (mouse); pY575R576: Biotin-SAPTSGpYREFVHAVE (human), PAPAGGpYREFVQAVKQ (mouse). The peptides were incubated with whole splenocyte lysates and avidin-conjugated magnetic beads overnight. The beads were then separated by magnetic sorting and washed. The bound proteins were eluted and analyzed using SDS-PAGE and immunoblotting [11,60].

Methylation analysis

The methylation status of the Foxp3 T_{reg} cell–specific demethylation region (CNS2) of WT Foxp3^{+}, *Il4ra*[R576] Foxp3^{+}CCR6^{−} and *Il4ra*[R576] Foxp3^{+}CCR6^{+} lung T_{reg} cells of OVA-sensitized and challenged mice was assessed by bisulfite sequence analysis, as described [61]. The T_{reg} cell-specific demethylation region of converted DNA was amplified with methylation-specific primer sequences: Foxp3 CNS2, 5'-TATTTTTTTGGGTTTTGGGATATTA-3' (forward) and Foxp3 CNS2 5'-AACCAACCAACTTCCTACACTATCTAT-3' (Reverse). The PCR product was subcloned and sequenced. Blast analyses were done by comparison of the resulting sequences with converted Foxp3 sequences.

In vitro suppression assays

Total CD4^{+} T cells were isolated using a CD4 negative isolation kit (Miltenyi Biotec) followed by cell sorting on FACSAria. Isolated cells were labeled with CellTrace Violet Cell Proliferation dye according to the manufacturer's instructions (Life Technologies) and were used as responder cells. T_{reg} cells were isolated on a FACSAria on the basis of CD4, EGFP and/or CCR6 expression and were used as suppressor cells. Responder cells were co-cultured with T_{reg} cells, at the indicated ratios, and stimulated for 3 days with 2 μg/ml of soluble anti-CD3 and 5 μg/ml of soluble anti-CD28 in 96-well, round-bottomed plates in triplicates. The cells were then analyzed for CellTrace dye dilution by flow cytometry.

Transcriptome profiling

CCR6^{−} or CCR6^{+} CD4^{+}EGFP^{+}T_{reg} cells were isolated by FACS from total lung digests of OVA-sensitized and challenged *Il4ra*[R576] mice. Total RNA was extracted using TRIzol reagent (Invitrogen) and converted into Double-stranded DNA (dsDNA), using SMART-Seq v4 Ultra Low Input RNA kit (Clontech). dsDNA was then fragmented to 200-300 bp size, using M220 Focused-ultrasonicator (Covaris), and utilized for construction of libraries for Illumina sequencing using KAPA Hyper Prep Kit (Kapa Biosystems). Libraries were then quantified using Qubit dsDNA HS (High Sensitivity) Assay Kit on Agilent High Sensitivity DNA Bioanalyzer.

RNA sequencing data was demultiplexed using perfect matches to indices and quality inspected using FastQC. The sequencing data was aligned to the mm10 build (Gencode annotation) of the mouse genome using STAR [62], and counts were quantified using HTSeq [63]. Raw counts were filtered for non-mitochondrial protein-coding genes with at least 3 counts in one sample, and were normalized using the DESeq2 package in R [64]. Pairwise comparisons of differential gene expression were computed using DESeq2.

Human cell studies

Asthmatic subjects and healthy controls were recruited under protocols approved by the Institutional Review Board at Boston Children's Hospital. The demographic details of the respective groups are described in Supplemental Tables 2 and 3. Asthmatic subjects, age range 6-47 years, were identified as having intermittent asthma or persistent mild, moderate to severe asthma following the classification of The National Asthma Education and Prevention Program: Expert Panel Report 3 [65]. Inclusion Criteria for Asthma included

current doctor's diagnosis of asthma, and ≥12 % FEV1 bronchodialtor reversibility or airway hyperresponsiveness reflected by a methacholine PC20 ≤16 mg/ml. Healthy control subjects were recruited with no medical history of asthma. Informed consent was obtained from all participants prior to blood collection. Blood samples were used for isolation of DNA using DNeasy Blood & Tissue Kit (Qiagen) for genotyping. Mutation detection was carried out using amplification resistance mutation screen (ARMS) PCR method with the following primers: Common Oligo: 5'-CCAGAGTCCAGACAACCTGACTTGCAAGAGAC-3'; Q576-specific: 5'-TGGGTGCCACCCTGCTCCACCGCATGTACAAACTCAT-3'; R576-specific: 5'-TGGGTGCCACCCTGCTCCACCGCATGTACAAACTCAC-3' [66]. For iT$_{reg}$ cell differentiation, peripheral blood mononuclear cells (PBMC) were isolated and naïve CD4$^+$CDRA$^+$CDRO$^-$T cells were derived by magnetic separation (Miltenyi biotech). The Isolated T cells were differentiated into iT$_{reg}$ differentiation as described for murine study and directly used for intracellular cytokine and FOXP3 expression analysis, using flow cytometry.

Statistical analysis

Statistical analyses were performed using GraphPad Prism 6 software (GraphPad), and employing the statistical tests indicated in the individual figure legends. Samples size was selected based on previous experiments. No samples were excluded. The investigators were blinded as to scoring the lung histopathology in individual experiments. *P* values of <0.05 were considered significant; n.s.: not significant. All error bars represent s.e.m. as noted in the individual figure legends. Unless otherwise stated, ≥2 independent experiments were carried out for all assays, and the displayed figures are representative of the obtained results. Comparisons between the average severity scores and ages between asthmatics subjects homozygous for IL4RA Q576 versus those heterozygous and homozygous for the IL4RA R576 were carried out using Student's unpaired two-tailed t-test. The sex distribution between those two groups was compared using Fisher's exact test.

Supplementary Material

Refer to Web version on PubMed Central for supplementary material.

Acknowledgements

References

1. Lambrecht BN, Hammad H. The immunology of asthma. Nat Immunol. 2015; 16:45–56. [PubMed: 25521684]

2. Mamessier E, et al. T-cell activation during exacerbations: a longitudinal study in refractory asthma. Allergy. 2008; 63:1202–1210. [PubMed: 18699937]

3. Hartl D, et al. Quantitative and functional impairment of pulmonary CD4+CD25hi regulatory T cells in pediatric asthma. J Allergy Clin Immunol. 2007; 119:1258–1266. [PubMed: 17412402]

4. Lloyd CM, Hawrylowicz CM. Regulatory T cells in asthma. Immunity. 2009; 31:438–449. [PubMed: 19766086]

5. Dominguez-Villar M, Baecher-Allan CM, Hafler DA. Identification of T helper type 1-like, Foxp3+ regulatory T cells in human autoimmune disease. Nat Med. 2011; 17:673–675. [PubMed: 21540856]

6. Krishnamoorthy N, et al. Early infection with respiratory syncytial virus impairs regulatory T cell function and increases susceptibility to allergic asthma. Nat Med. 2012; 18:1525–1530. [PubMed: 22961107]

7. Komatsu N, et al. Pathogenic conversion of Foxp3+ T cells into TH17 cells in autoimmune arthritis. Nat Med. 2014; 20:62–68. [PubMed: 24362934]

8. Oldenhove G, et al. Decrease of Foxp3+ Treg cell number and acquisition of effector cell phenotype during lethal infection. Immunity. 2009; 31:772–786. [PubMed: 19896394]

9. Noval Rivas M, et al. Regulatory T Cell Reprogramming toward a Th2-Cell-like Lineage Impairs Oral Tolerance and Promotes Food Allergy. Immunity. 2015; 42:512–523. [PubMed: 25769611]

10. Gour N, Wills-Karp M. IL-4 and IL-13 signaling in allergic airway disease. Cytokine. 2015

11. Tachdjian R, et al. In vivo regulation of the allergic response by the IL-4 receptor alpha chain immunoreceptor tyrosine-based inhibitory motif. J Allergy Clin Immunol. 2010; 125:1128–1136. e1128. [PubMed: 20392476]

12. Chatila TA. Interleukin-4 receptor signaling pathways in asthma pathogenesis. Trends Mol Med. 2004; 10:493–499. [PubMed: 15464449]

13. Hershey GK, Friedrich MF, Esswein LA, Thomas ML, Chatila TA. The association of atopy with a gain-of-function mutation in the alpha subunit of the interleukin-4 receptor. N Engl J Med. 1997; 337:1720–1725. [PubMed: 9392697]

14. Wenzel SE, et al. IL4R alpha mutations are associated with asthma exacerbations and mast cell/IgE expression. Am J Respir Crit Care Med. 2007; 175:570–576. [PubMed: 17170387]

15. Rosa-Rosa L, Zimmermann N, Bernstein JA, Rothenberg ME, Khurana Hershey GK. The R576 IL-4 receptor alpha allele correlates with asthma severity. J Allergy Clin Immunol. 1999; 104:1008–1014. [PubMed: 10550746]

16. Al-Muhsen S, et al. IL-4 receptor alpha single-nucleotide polymorphisms rs1805010 and rs1801275 are associated with increased risk of asthma in a Saudi Arabian population. Annals of thoracic medicine. 2014; 9:81–86. [PubMed: 24791170]

17. Tachdjian R, et al. Pathogenicity of a disease-associated human IL-4 receptor allele in experimental asthma. J Exp Med. 2009; 206:2191–2204. [PubMed: 19770271]

18. Xia M, et al. Vehicular exhaust particles promote allergic airway inflammation through an aryl hydrocarbon receptor-notch signaling cascade. J Allergy Clin Immunol. 2015

19. Ryan JJ, McReynolds LJ, Huang H, Nelms K, Paul WE. Characterization of a mobile Stat6 activation motif in the human IL-4 receptor. J Immunol. 1998; 161:1811–1821. [PubMed: 9712048]

20. Wang HY, et al. Cutting edge: effects of an allergy-associated mutation in the human IL-4R alpha (Q576R) on human IL-4-induced signal transduction. J Immunol. 1999; 162:4385–4389. [PubMed: 10201973]

21. Al-Ramli W, et al. T(H)17-associated cytokines (IL-17A and IL-17F) in severe asthma. J Allergy Clin Immunol. 2009; 123:1185–1187. [PubMed: 19361847]

22. Wang YH, et al. A novel subset of CD4(+) T(H)2 memory/effector cells that produce inflammatory IL-17 cytokine and promote the exacerbation of chronic allergic asthma. J Exp Med. 2010; 207:2479–2491. [PubMed: 20921287]

23. Cosmi L, et al. Identification of a novel subset of human circulating memory CD4(+) T cells that produce both IL-17A and IL-4. J Allergy Clin Immunol. 2010; 125:222–230. e221–224. [PubMed: 20109749]

24. Irvin C, et al. Increased frequency of dual-positive TH2/TH17 cells in bronchoalveolar lavage fluid characterizes a population of patients with severe asthma. J Allergy Clin Immunol. 2014; 134:1175–1186. e1177. [PubMed: 25042748]

25. Thornton AM, et al. Expression of Helios, an Ikaros transcription factor family member, differentiates thymic-derived from peripherally induced Foxp3+ T regulatory cells. J Immunol. 2010; 184:3433–3441. [PubMed: 20181882]

26. Hirota K, et al. Preferential recruitment of CCR6-expressing Th17 cells to inflamed joints via CCL20 in rheumatoid arthritis and its animal model. J Exp Med. 2007; 204:2803–2812. [PubMed: 18025126]

27. Duhen T, Duhen R, Lanzavecchia A, Sallusto F, Campbell DJ. Functionally distinct subsets of human FOXP3+ Treg cells that phenotypically mirror effector Th cells. Blood. 2012; 119:4430–4440. [PubMed: 22438251]

28. Chen W, et al. Conversion of peripheral CD4+CD25- naive T cells to CD4+CD25+ regulatory T cells by TGF-beta induction of transcription factor Foxp3. J Exp Med. 2003; 198:1875–1886. [PubMed: 14676299]

29. Weiss JM, et al. Neuropilin 1 is expressed on thymus-derived natural regulatory T cells, but not mucosa-generated induced Foxp3+ T reg cells. J Exp Med. 2012; 209:1723–1742. S1721. [PubMed: 22966001]

30. Yadav M, et al. Neuropilin-1 distinguishes natural and inducible regulatory T cells among regulatory T cell subsets in vivo. J Exp Med. 2012; 209:1713–1722. S1711–1719. [PubMed: 22966003]

31. Yosef N, et al. Dynamic regulatory network controlling TH17 cell differentiation. Nature. 2013; 496:461–468. [PubMed: 23467089]

32. Yu X, et al. TH17 cell differentiation is regulated by the circadian clock. Science. 2013; 342:727–730. [PubMed: 24202171]

33. Hou L, et al. The protease cathepsin L regulates Th17 cell differentiation. Journal of autoimmunity. 2015; 65:56–63. [PubMed: 26343333]

34. Kessels HW, Ward AC, Schumacher TN. Specificity and affinity motifs for Grb2 SH2-ligand interactions. Proc Natl Acad Sci U S A. 2002; 99:8524–8529. [PubMed: 12084912]

35. Rojas JM, Oliva JL, Santos E. Mammalian son of sevenless Guanine nucleotide exchange factors: old concepts and new perspectives. Genes & cancer. 2011; 2:298–305. [PubMed: 21779500]

36. Ray A, Prefontaine KE. Physical association and functional antagonism between the p65 subunit of transcription factor NF-kappa B and the glucocorticoid receptor. Proc Natl Acad Sci U S A. 1994; 91:752–756. [PubMed: 8290595]

37. Vanden Berghe W, et al. Signal transduction by tumor necrosis factor and gene regulation of the inflammatory cytokine interleukin-6. Biochemical pharmacology. 2000; 60:1185–1195. [PubMed: 11007957]

38. Bettelli E, et al. Reciprocal developmental pathways for the generation of pathogenic effector TH17 and regulatory T cells. Nature. 2006; 441:235–238. [PubMed: 16648838]

39. Yang XO, et al. STAT3 regulates cytokine-mediated generation of inflammatory helper T cells. J Biol Chem. 2007; 282:9358–9363. [PubMed: 17277312]

40. Maneechotesuwan K, et al. Regulation of Th2 cytokine genes by p38 MAPK- mediated phosphorylation of GATA-3. J Immunol. 2007; 178:2491–2498. [PubMed: 17277157]

41. Saleh A, Shan L, Halayko AJ, Kung S, Gounni AS. Critical role for STAT3 in IL-17A-mediated CCL11 expression in human airway smooth muscle cells. J Immunol. 2009; 182:3357–3365. [PubMed: 19265112]

42. Mathew A, et al. Signal transducer and activator of transcription 6 controls chemokine production and T helper cell type 2 cell trafficking in allergic pulmonary inflammation. J Exp Med. 2001; 193:1087–1096. [PubMed: 11342593]

43. Hoshino A, et al. STAT6-mediated signaling in Th2-dependent allergic asthma: critical role for the development of eosinophilia, airway hyper-responsiveness and mucus hypersecretion, distinct from its role in Th2 differentiation. Int Immunol. 2004; 16:1497–1505. [PubMed: 15351784]

44. Ivanov II, et al. The orphan nuclear receptor RORgammat directs the differentiation program of proinflammatory IL-17+ T helper cells. Cell. 2006; 126:1121–1133. [PubMed: 16990136]

45. Ford AQ, Heller NM, Stephenson L, Boothby MR, Keegan AD. An atopy-associated polymorphism in the ectodomain of the IL-4R(alpha) chain (V50) regulates the persistence of STAT6 phosphorylation. J Immunol. 2009; 183:1607–1616. [PubMed: 19592641]

46. Stephenson L, Johns MH, Woodward E, Mora AL, Boothby M. An IL-4R alpha allelic variant, I50, acts as a gain-of-function variant relative to V50 for Stat6, but not Th2 differentiation. J Immunol. 2004; 173:4523–4528. [PubMed: 15383584]

47. Kudo M, et al. IL-17A produced by alphabeta T cells drives airway hyper- responsiveness in mice and enhances mouse and human airway smooth muscle contraction. Nat Med. 2012; 18:547–554. [PubMed: 22388091]

48. McKinley L, et al. TH17 cells mediate steroid-resistant airway inflammation and airway hyperresponsiveness in mice. J Immunol. 2008; 181:4089–4097. [PubMed: 18768865]

49. Woodruff PG, et al. T-helper type 2-driven inflammation defines major subphenotypes of asthma. Am J Respir Crit Care Med. 2009; 180:388–395. [PubMed: 19483109]

50. Bhakta NR, Erle DJ. IL-17 and "TH2-high" asthma: Adding fuel to the fire? J Allergy Clin Immunol. 2014; 134:1187–1188. [PubMed: 25174869]

51. Muraro A, et al. Precision medicine in patients with allergic diseases: Airway diseases and atopic dermatitis-PRACTALL document of the European Academy of Allergy and Clinical Immunology and the American Academy of Allergy, Asthma & Immunology. J Allergy Clin Immunol. 2016; 137:1347–1358. [PubMed: 27155030]

52. Wenzel S, et al. Dupilumab in persistent asthma with elevated eosinophil levels. N Engl J Med. 2013; 368:2455–2466. [PubMed: 23688323]

53. Samson M, et al. Brief report: inhibition of interleukin-6 function corrects Th17/Treg cell imbalance in patients with rheumatoid arthritis. Arthritis Rheum. 2012; 64:2499–2503. [PubMed: 22488116]

Methods-only References

54. Haribhai D, et al. Regulatory T cells dynamically control the primary immune response to foreign antigen. J Immunol. 2007; 178:2961–2972. [PubMed: 17312141]

55. Zhou X, et al. Selective miRNA disruption in T reg cells leads to uncontrolled autoimmunity. J Exp Med. 2008; 205:1983–1991. [PubMed: 18725525]

56. Voehringer D, Wu D, Liang HE, Locksley RM. Efficient generation of long- distance conditional alleles using recombineering and a dual selection strategy in replicate plates. BMC biotechnology. 2009; 9:69. [PubMed: 19638212]

57. Rubtsov YP, et al. Regulatory T cell-derived interleukin-10 limits inflammation at environmental interfaces. Immunity. 2008; 28:546–558. [PubMed: 18387831]

58. McFarland-Mancini MM, et al. Differences in wound healing in mice with deficiency of IL-6 versus IL-6 receptor. J Immunol. 2010; 184:7219–7228. [PubMed: 20483735]

59. Blaeser F, et al. Targeted Inactivation of the IL-4 Receptor Chain I4R Motif Promotes Allergic Airway Inflammation. J Exp Med. 2003; 198:1189–1200. [PubMed: 14557412]

60. Carrera P, Righetti PG, Gelfi C, Ferrari M. Amplification refractory mutation system analysis of point mutations by capillary electrophoresis. Methods in molecular biology. 2001; 163:95–108. [PubMed: 11242967]

61. Charbonnier LM, Wang S, Georgiev P, Sefik E, Chatila TA. Control of peripheral tolerance by regulatory T cell-intrinsic Notch signaling. Nat Immunol. 2015; 16:1162–1173. [PubMed: 26437242]

62. Dobin A, et al. STAR: ultrafast universal RNA-seq aligner. Bioinformatics. 2013; 29:15–21. [PubMed: 23104886]

63. Anders S, Pyl PT, Huber W. HTSeq--a Python framework to work with high- throughput sequencing data. Bioinformatics. 2015; 31:166–169. [PubMed: 25260700]

64. Love MI, Huber W, Anders S. Moderated estimation of fold change and dispersion for RNA-seq data with DESeq2. Genome Biol. 2014; 15:550. [PubMed: 25516281]

65. National Asthma E, Prevention P. Expert Panel Report 3 (EPR-3): Guidelines for the Diagnosis and Management of Asthma-Summary Report 2007. J Allergy Clin Immunol. 2007; 120:S94–138. [PubMed: 17983880]

66. Little S. Amplification-refractory mutation system (ARMS) analysis of point mutations. Current protocols in human genetics / editorial board, Jonathan L. Haines ... [et al. 2001 Chapter 9, Unit 9 8.
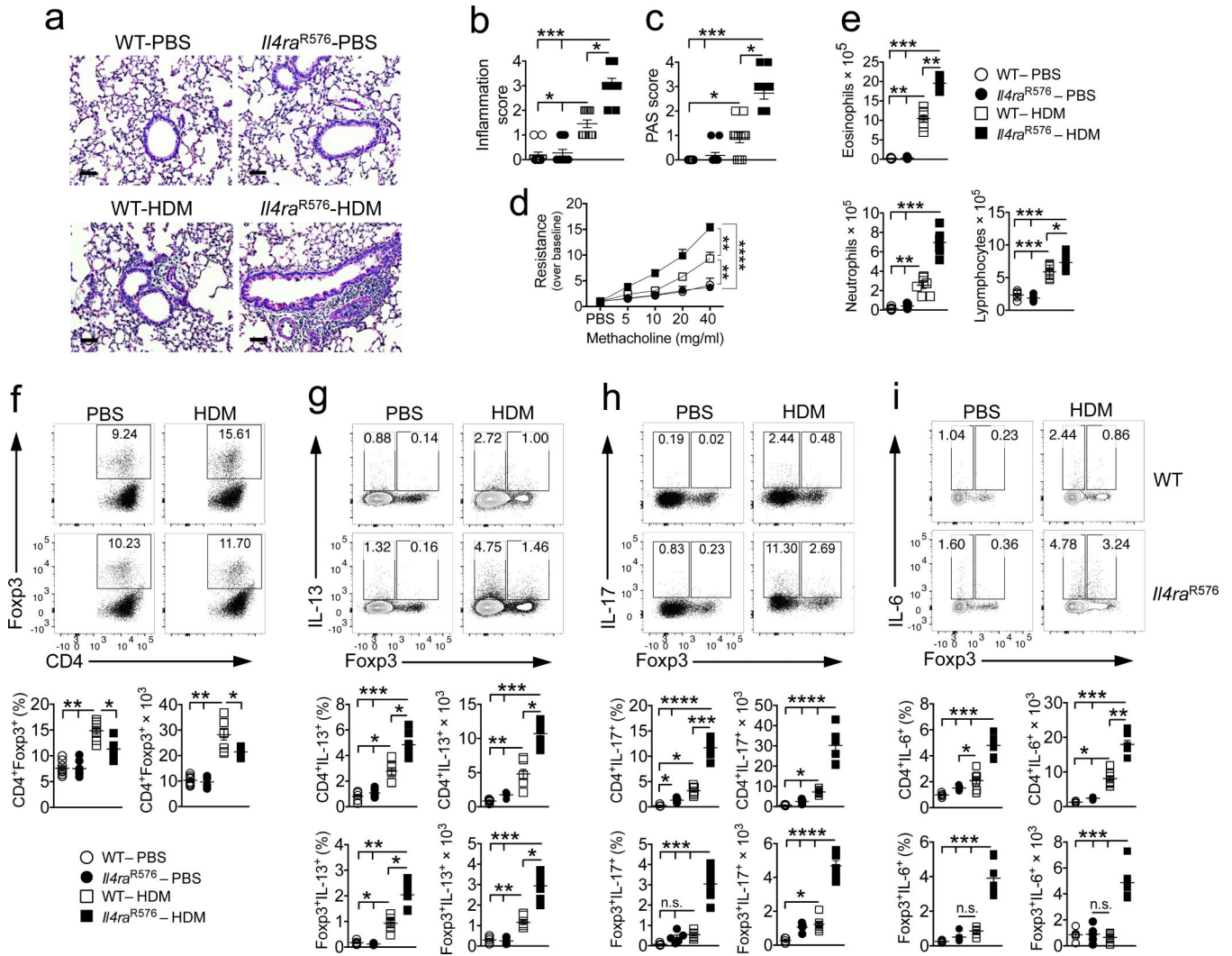
Figure 1.
Il4ra[R576] polymorphism promotes enhanced lung inflammation and AHR, associated with increased IL-17, IL-6 and IL-13 expression. (**a**) Representative PAS staining of lung sections isolated from WT and *Il4ra*[R576] mice either sham treated with PBS or immunized and challenged with HDM and analyzed 24 hr after the last challenge (20×, scale bar 50 μm) (*n* = 11 counts per field-of-view). (**b,c**) Inflammation and PAS scores from the group of mice shown in **a**. (**d**) Methacholine–induced AHR for the same groups shown in **a** (*n* = 8 mice per group). (**e**) Absolute numbers of lung tissue eosinophils, neutrophils and lymphocytes, in the respective mouse groups (*n* = 5 mice for PBS and 7 mice for HDM groups). (**f**) Flow cytometric analysis, frequencies and absolute numbers of CD4+Foxp3+ T$_{reg}$ cells within lung tissue (*n* = 8 mice per group). (**g–i**) Flow cytometric analysis of IL-13 (**g**), IL-17 (**h**) and IL-6 (**i**) expression by CD4+Foxp3− T$_{conv}$ or CD4+Foxp3+ T$_{reg}$ cells within CD90.2+ gated cells (representing all T lymphocytes) in lung tissues of WT and *Il4ra*[R576] mice treated with PBS or HDM (*n* = 5 mice for PBS and 7 mice for HDM groups). Results represent means ± s.e.m. from two independent experiments. *$P < 0.05$, **$P < 0.01$ and ***$P < 0.001$

by one-way ANOVA with Bonferroni posttest analysis. For AHR analysis, $*P < 0.05$ and $**P < 0.01$ by two-way repeated measures ANOVA.
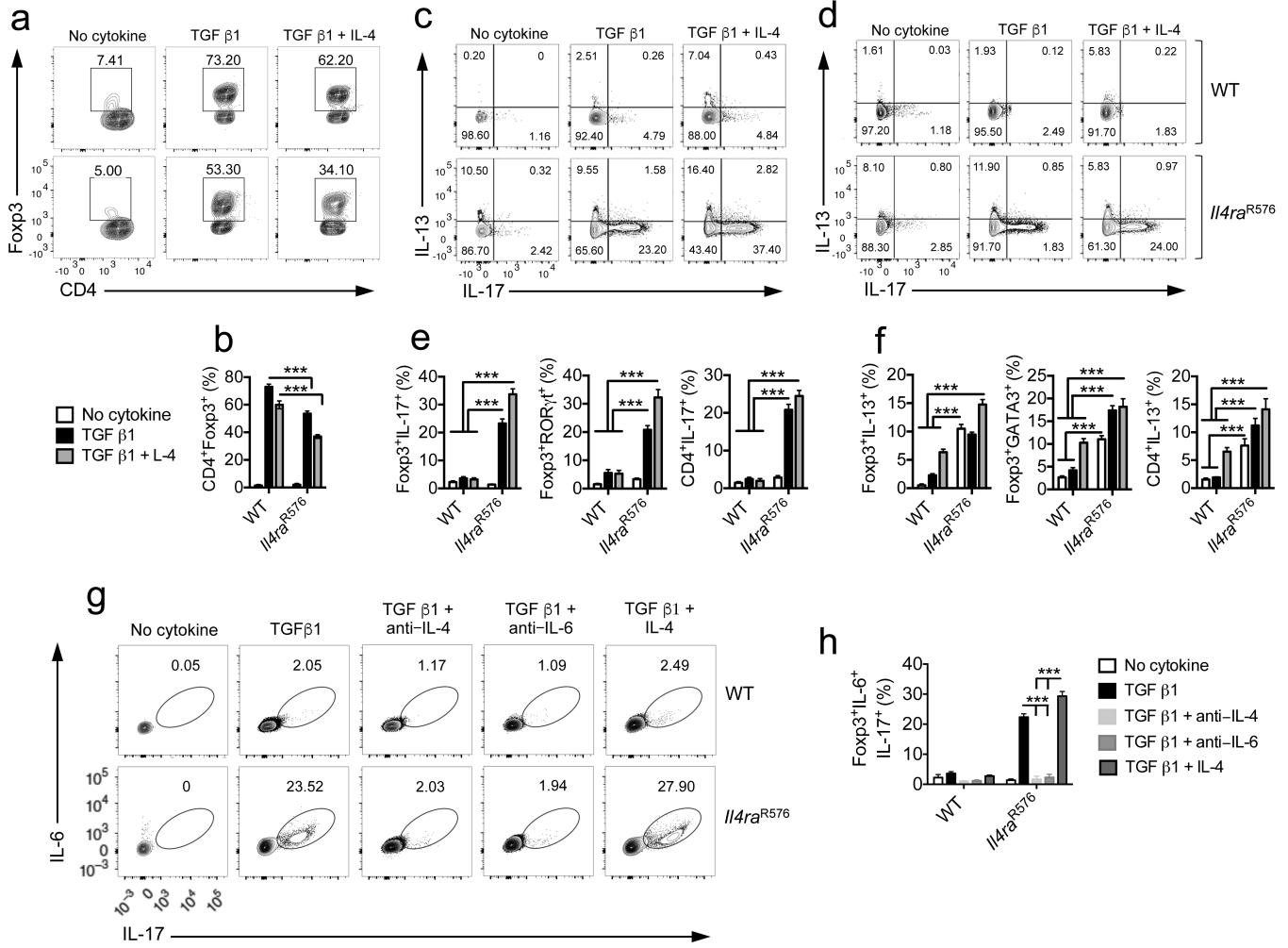
Figure 2.
Defective formation and impaired suppressive function of $Il4ra^{R576}$ induced-T_{reg} cells. (**a,b**) Flow cytometric plot (**a**) and bar graph (**b**) demonstrating *in vitro* generation of iT_{reg} cells form $DO11.10^+Rag2^{-/-}Foxp3^{EGFP}$ and $DO11.10^+Il4ra^{R576}Rag2^{-/-}Foxp3^{EGFP}$ naïve CD4$^+$ T_{conv} cells in the presence of anti-CD3 and anti–CD28 mAbs and TGF β1 in the absence or presence of IL-4 for 5 d ($n = 6$ replicates per group). (**c,d**) Flow cytometric analysis of IL-17 and IL-13 expression by converted Foxp3$^+$ iT_{reg} cells (**c**) and CD4$^+$Foxp3$^-$ T_{conv} cells (**d**) in culture. (**e,f**) Bar graphs demonstrating the frequencies of converted Foxp3$^+$ iT_{reg} and CD4$^+$Foxp3$^-$ T_{conv} cells IL-17 and RORγt (**e**) and IL-13 and GATA3 expression (**f**) ($n = 6$ replicates for IL-17 and IL-13 and 6 replicates for RORγt and GATA3 expression). (**g**) Flow cytometric analysis of dual IL-6 and IL-17 expression by converted iT_{reg} cells. (**h**) Bar graph demonstrating the frequencies of double IL-6 and IL-17 expression within converted iT_{reg} cells ($n = 6$ replicates per group). Each dot represents one replicate. Data represent means ± s.e.m. from two independent experiments. ***P < 0.001 by one-way ANOVA with Bonferroni posttest analysis.
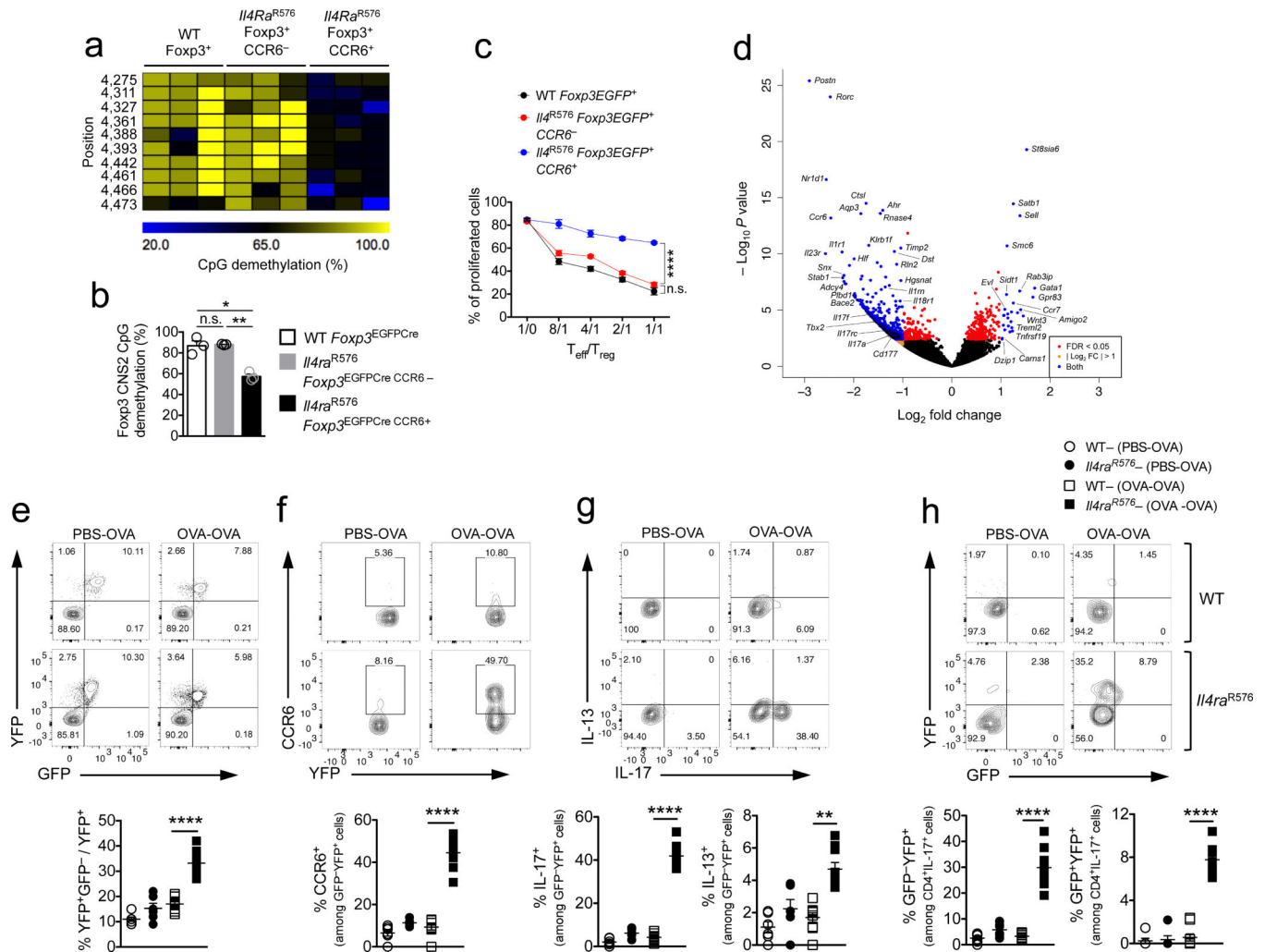
Figure 3.
CCR6+ IL-17+ *Il4*R576 T_reg cells exhibit instability and compromised suppressive activity (**a**) Methylation status of CpG motifs in T_reg cells isolated from lung tissue of OVA–sensitized and challenged mice. Numbers on the left side indicate the position of the respective motifs. (**b**) Global methylation status of *Foxp3* CNS2 in the respective T_reg cell populations ($n = 3$ mice per group with 7-12 clones per mouse). (**c**) *In vitro* suppression of the proliferation of WT responder CD4+ T cells (T_eff) by the respective T_reg cell populations ($n = 3$ replicates per group) (**d**) Gene expression profiles (volcano plot) of EGFP+CCR6− versus EGFP+CCR6+ T_reg cells isolated by FACS from lung digests of OVA-sensitized and challenged *Foxp3*EGFP *Il4*R576 mice ($n = 3$–4 mice). FDR: false discovery rate; Log_2FC: Log_2 fold change. (**e**) Flow cytometric analysis and frequencies of exT^reg (GFP−YFP+) cells, plotted as a fraction of exT_reg to total T_reg cells in lung tissue. (**f,g**) Flow cytometric analysis and frequencies of CCR6 producing (**f**) and IL-17 and IL-13 producing (**g**) exT_reg cells in lung tissues. (**h**) Flow cytometric analysis and frequencies of exT_reg and T_reg cells among CD4+IL-17+ T_conv cells in lung tissues of the respective mouse groups ($n = 6$ mice for PBS- and 9 mice for OVA-treated groups for **e–h**). Data represent means ± s.e.m. from two independent experiments. $*P < 0.05$, $**P < 0.005$ and $****P < 0.0001$ by one-way ANOVA

with Bonferroni posttest analysis. For suppression assay ****P < 0.0001 by repeated measures two-way ANOVA.
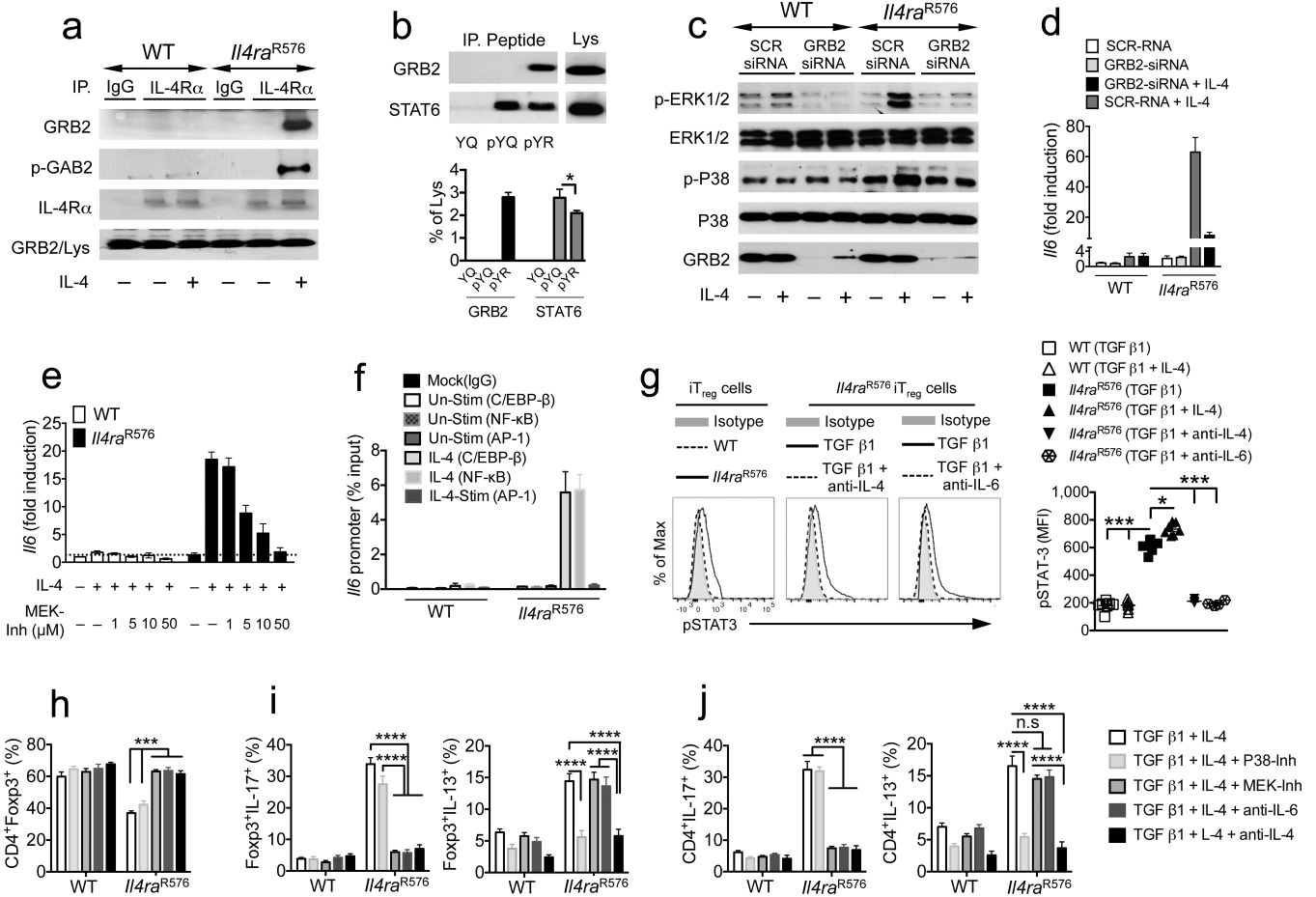
Figure 4.

IL-4Rα-R576 activates GRB2–coupled MAPK. (**a**) Immunoprecipitates (IP) from medium and IL-4-treated WT and $Il4ra^{R576}$ splenocytes using IgG or anti–IL4Rα mAb were probed with anti-GRB2, -GAB2, and -IL-4Rα mAbs. Lys: lysates (**b**) Binding of GRB2 and STAT6 in splenocyte lysates to biotinylated murine IL-4Rα Y575Q576 (YQ), pY575Q576 (pYQ) and pY575R576 (pYR) peptides. Immunoblotted proteins (upper panel) were quantified by densitometry (lower panel). (**c**) Immunoblots of phospho- and total ERK1/2 and p38, and of GRB2 in medium or IL-4–treated WT and $Il4ra^{R576}$ BMDM transfected with scrambled or GRB2–specific siRNA. (**d**) RT-PCR analysis of $Il6$ transcripts in the same groups as **c** (**e**) $Il6$ transcripts in splenocytes treated with medium or IL-4 and the indicated concentrations of MEK-Inh. (**f**) ChIP analysis of C/EBP-β, NF-κB and AP-1 binding at the $Il6$ promoter in medium (Un-Stim) or IL-4–treated WT and $Il4ra^{R576}$ splenocytes. (**g**) Flow cytomeric analysis (left) and mean fluorescence intensity (MFI, right) of pSTAT3 in WT and $Il4ra^{R576}$ iT$_{reg}$ cells differentiated with anti–CD3, anti–C28 mAbs and TGF β1 without or with IL-4, anti-IL-4 or anti–IL-6 mAbs ($n = 3$–6 replicates per group for **b–g**). (**h–j**) Frequencies of iT$_{reg}$ cells (**h**) IL-17 and IL-13 expressing Foxp3$^+$ iT$_{reg}$ cells (**i**) and CD4$^+$Foxp3$^-$ T$_{conv}$ cells (**j**) treated with the indicated combinations of cytokines, inhibitors and mAbs ($n = 3$–6 replicates per group). Data represent means ± s.e.m. from 2–3 independent experiments. $*P$

< 0.05, ***P < 0.001 and ****P < 0.0001 by one-way ANOVA with Bonferroni posttest analysis.
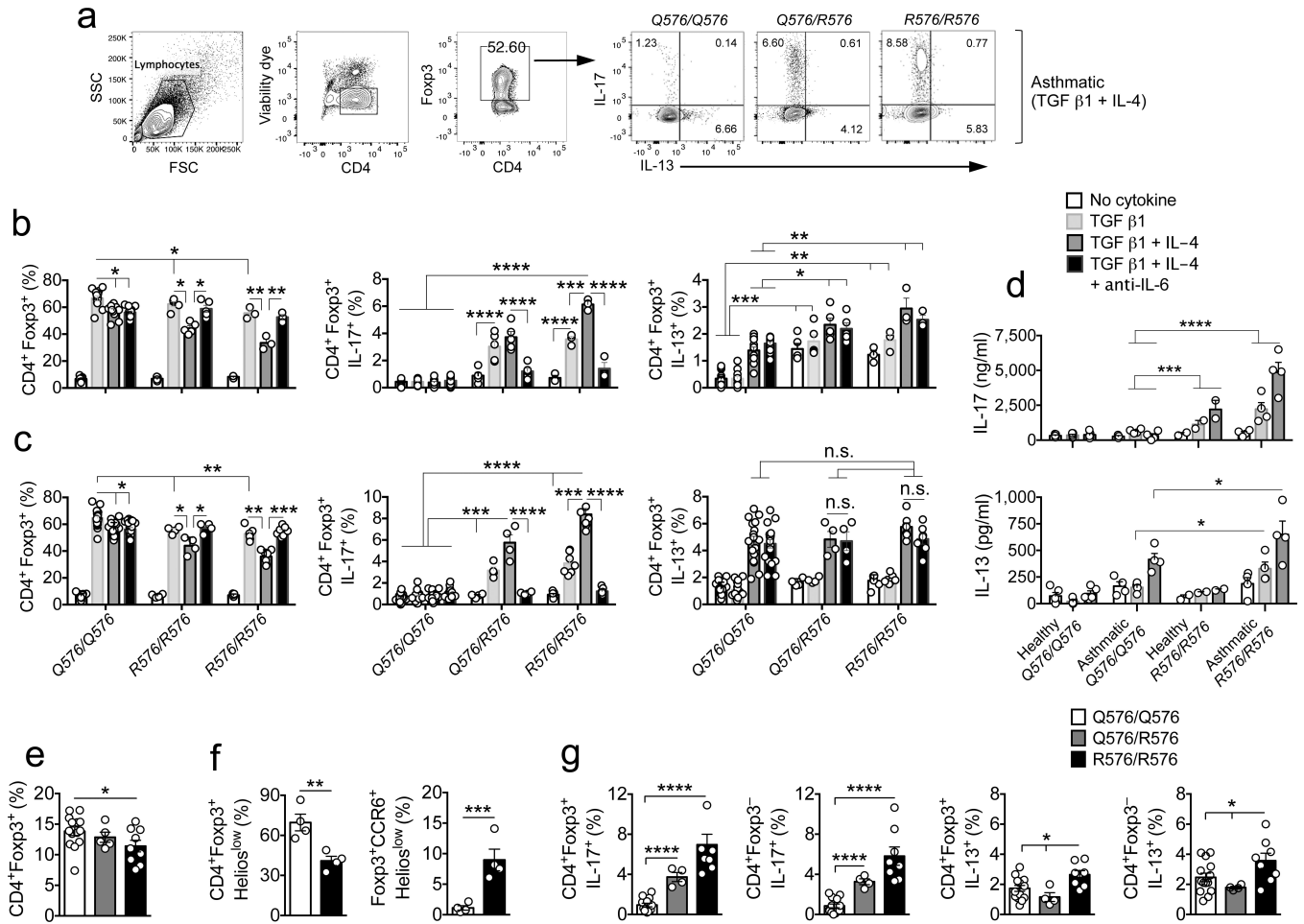
Figure 5.
Naïve CD4$^+$ T$_{conv}$ cells from asthmatic subjects bearing R576 mutation show defective induction of iT$_{reg}$ cells and their skewing towards a T$_H$17-like phenotype. (**a**) Flow cytometric analysis of CD4$^+$Foxp3$^+$ iT$_{reg}$ cells induced from purified naïve CD4$^+$ T$_{conv}$ in the presence of anti-CD3 + anti-CD28 mAbs and TGF β1 + IL-4 in the absence or presence of anti-IL-6 mAb. (**b,c**) Cumulative frequencies of CD4$^+$Foxp3$^+$ iT$_{reg}$ cells and IL-17 and IL-13 producing Foxp3$^+$ iT$_{reg}$ cells within converted iT$_{reg}$ cells of non-asthmatic ($n = 3–13$) (**b**) and asthmatic ($n = 4–19$) (**c**) subjects with respective genotypes differentiated in the absence or presence of TGF β1 or TGF β1 + IL-4 or TGF β1 + IL-4 + anti-IL-6 mAb. (**d**) IL-17 and IL-13 cytokine levels in the supernatant of differentiated iT$_{reg}$ cells in the treated groups mentioned in **b** ($n = 2–5$). (**e-g**) Frequencies of total CD4$^+$Foxp3$^+$ T$_{reg}$ cells ($n = 5–$14) (**e**) CD4$^+$Foxp3$^+$Helios^{low} and Foxp3$^+$CCR6$^+$Helios^{low} T$_{reg}$ cells ($n = 4$) (**f**) and frequencies of IL-17 and IL-13 producing Foxp3$^+$ T$_{reg}$ and CD4$^+$ T$_{conv}$ cells in respective groups within PBMC of asthmatic subjects ($n = 4–14$). Each dot represents one subject. Data represent means ± s.e.m. For subjects see Supplementary Tables 2 and 3. *$P < 0.05$, **$P < 0.01$, ***$P < 0.001$ and ****$P < 0.001$ by one-way ANOVA with Bonferroni posttest analysis.
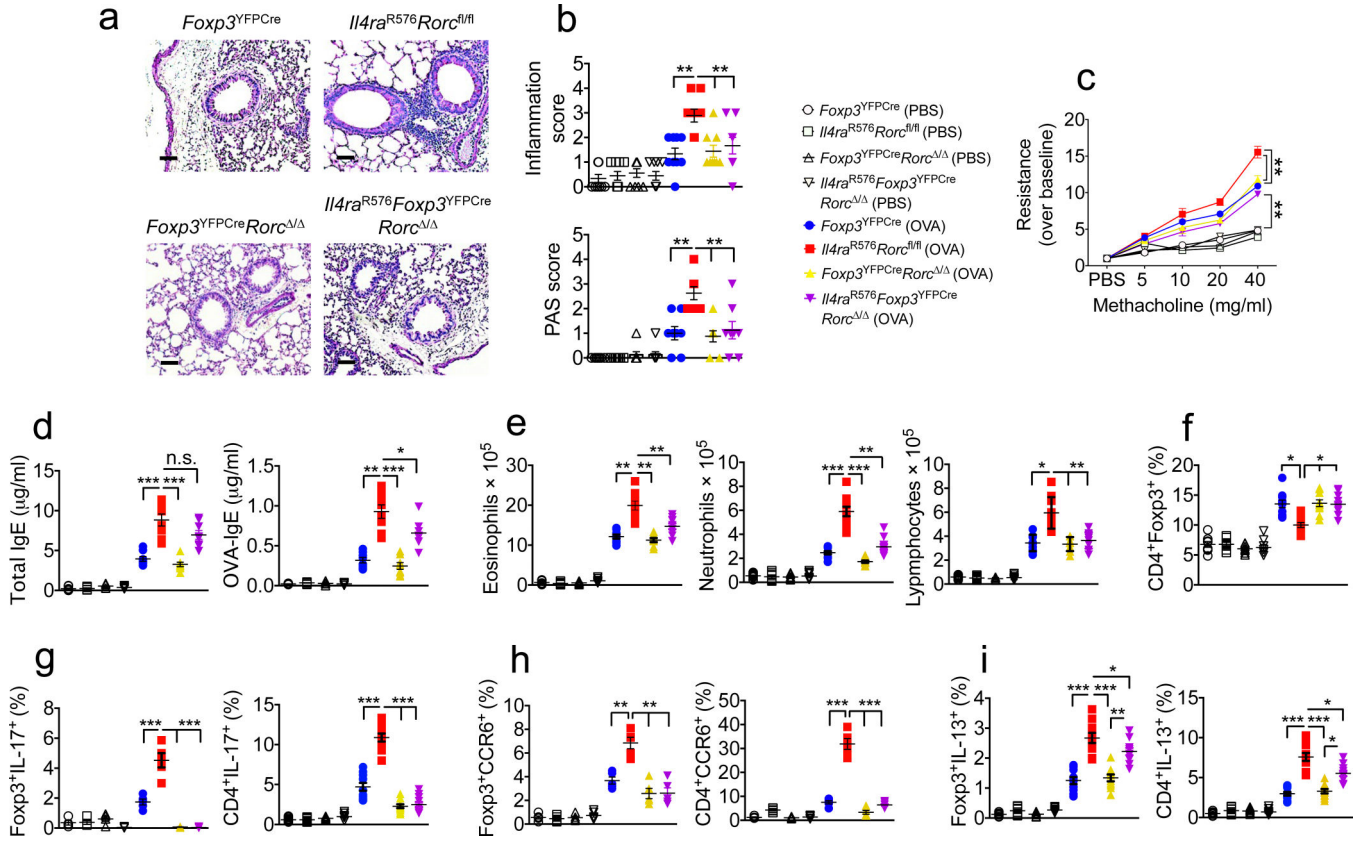
Figure 6.

T_reg cell lineage-specific deletion of *Rorc* reverses the aggravated airway inflammation in *Il4ra*[R576] mice. (**a**) PAS staining of lung sections isolated from the mouse groups shown and immunized and challenged with OVA (20×, scale bar 50 μm). (**b**) Inflammation and PAS scores in the mouse groups shown ($n = 8$–9 counts per field of view). (**c**) Methacholine–induced AHR in the respective mouse groups ($n = 4$ mice for PBS- and 6 mice for OVA–treated mouse groups). (**d**) Total and OVA–specific serum IgE concentrations in the mouse groups shown in b ($n = 8$). (**e**) Frequencies of lung tissue eosinophils, neutrophils and lymphocytes ($n = 8$ mice for PBS- and 9 mice for OVA-treated mouse groups). (**f–i**) Frequencies of lung tissue Foxp3^{+} T_reg cells (**f**), and IL-17 (**g**), CCR6 (**h**) and IL-13 (**i**) producing CD4^{+} T^conv and Foxp3^{+} T_reg and CD4^{+} T_conv cells ($n = 5$–9 mice per group). Each dots represents one animal. Data represent means ± s.e.m. from two to three independent experiments. *$P<0.05$, **$P<0.01$, ***$P<0.001$ and ****$P<0.0001$ by one-way ANOVA with Bonferroni posttest analysis. For AHR studies, *$P< 0.05$ and **$P< 0.01$ by repeated measures two-way ANOVA.